OPTIMISATION OF SPEED TRAJECTORIES TO IMPROVE THE ENERGY ECONOMY OF ELECTRIC VEHICLES

(MSc Thesis ME57035)

Tushar Goyal

MSc Mechanical Engineering

Track: Vehicle Engineering

ID: 5220068

Under the supervision of:

Dr. Laura Ferranti

Dept: Cognitive Robotics

TU Delft Delft University of Technology

Dr. Mauro Salazar Villalon

&

Dr. Thijs van Keulen

Dept: Mechanical Engineering,

TU/e EINDHOVEN UNIVERSITY OF TECHNOLOGY

Table of Contents

Abstract

Electric vehicles are a cleaner and more efficient means of transport. However, the sub-energy-optimal acceleration and deceleration inputs of drivers result in speed trajectories that cause superfluous expenditure of the stored electrical energy in battery. Optimising the speed trajectories to minimise the consumption of stored energy is a potential strategy for the efficient operation of electric vehicles. In this thesis, we propose a numerical solution to the eco-driving problem by optimising the speed trajectories via Pontryagin's Minimum Principle. The solution is robust to the vehicle parameters and the driving conditions, and is used to generate energy-aware driving advice for near-straight line driving manoeuvres. In the end, we test the global optimality of the speed trajectories by convexification of the problem.

Keywords: Speed trajectory optimisation, Eco-driving, Pontryagin's minimum principle, Convex optimisation

Acknowledgement

For a period spanning two academic quarters, I have had the privilege to have Dr. Mauro Salazar supervise my thesis. He is a decorated professor with an immense enthusiasm for future vehicle technology. Right from finalising a relevant thesis topic, he has motivated to explore the field and accept challenging problems. Consequently, I have equipped myself with new tools and methodologies that have more general applications. Furthermore, he gave me access to the right reference material that taught me a great amount of scientific writing.

As a co-supervisor, Dr. Thijs van Keulen has expertise in optimal control theory and vehicle powertrains among other research interests. He has willingly shared his insightful knowledge and provided meticulous feedback for me to produce a quality output. This enabled me to think more critically and revise the work each time.

My internal supervisor and optimization-based algorithms expert, Dr. Laura Ferranti has diligently coordinated the thesis and gave me the necessary push to maintain the progress and abide by the timeline. This caused me to maintain consistency in my output.

For the last section of my thesis, I have had the opportunity to receive intelligent inputs from Olaf Borsboom who presently pursues Ph.D. at the Control Systems Technology Group of Eindhoven University of Technology. Meeting with him, I developed a broader perspective of the problem I studied for thesis.

I am thankful to my institute, Delft University of Technology, for giving me the access to its tools and resources which I have leveraged during my entire study.

Next, I owe my deepest gratitude to my family members who have unceasingly supported me at each stage. It has inspired me to put maximum effort and enjoy the process. I am forever grateful for their love, support, and belief in me.

My gratitude extends to my flatmates, Adwait Inamdar and Saloni Tomar who have been with me through my journey, shared their experiences and guided me as and when I hit roadblocks.

Warm thanks

1

Introduction

Among several efforts to decarbonise the planet, emission targets for original equipment manufacturers have been made stricter time and again worldwide. Transportation makes for the second largest sector in terms of the greenhouse gas emissions after the energy production [1]. To contain these emissions during the operation of vehicles, the automotive manufacturers are electrifying their range, seven of which including Mercedes-Benz, Volvo Cars and Bentley Motors Limited have already committed to 100% electric vehicle (EV) sales by 2030 within the European Union [2]. To reap the environmental benefits of EVs, their production as well as operation should be energy efficient. The energy consumption and emission tests are performed to quantify the operational efficiency using the driving cycles which are largely influenced by the driver inputs: acceleration and braking. However, the inputs are often aggressive and/ or sub-energy-optimal causing a higher expenditure of stored electrical energy in the battery than necessary. Hence, the on-road operation of EVs is not energy-optimal.

1.1 Eco-driving to Minimise Energy Consumption

Optimising the driver inputs for the desired trip duration and distance to be covered is one of the strategies to minimise the energy consumed for each trip. For this optimisation, eco-driving, an advanced driver-assistance system to improve the economy of stored energy in the form of combustible fuel or charge in the battery of on-road vehicles [3], is researched as well as implemented in different forms [4]. In [5], for the combustion and the hybrid EVs (HEVs), the fuel economy is defined as the amount of fuel consumed to travel a fixed distance, or, alternatively, the distance travelled for a fixed amount of fuel. For the EVs, the fuel economy corresponds to the economy of stored electrical energy in the battery, henceforth referred to as the *energy economy*. One of the ways the eco-driving system improves the energy economy is by modifying the driver inputs through a less responsive throttle tuning and transmission shift points. This decreases the responsiveness of the vehicle powertrain as illustrated in Fig. 1 thereby preventing aggressive accelerations and decelerations which rapidly deplete the stored energy. Note that the eco-driving mode does not limit the total output but only voids the unnecessary throttle input during moderate driving.

Another way the eco-driving system improves the energy economy is through the management of the auxiliary loads on the vehicle, the largest of which is air-conditioning [6]. By altering the operation of these loads, the eco-driving system enables a more conservative use of the available electrical energy from the battery of EVs. For the combustion vehicles, it has already been shown that along with the driver's practice of energy-aware driving style, which includes minimising idling, driving with sufficiently inflated tires etc, eco-driving system can cumulatively improve the fuel economy up to 45% [4]. Similarly, with the aim to improve

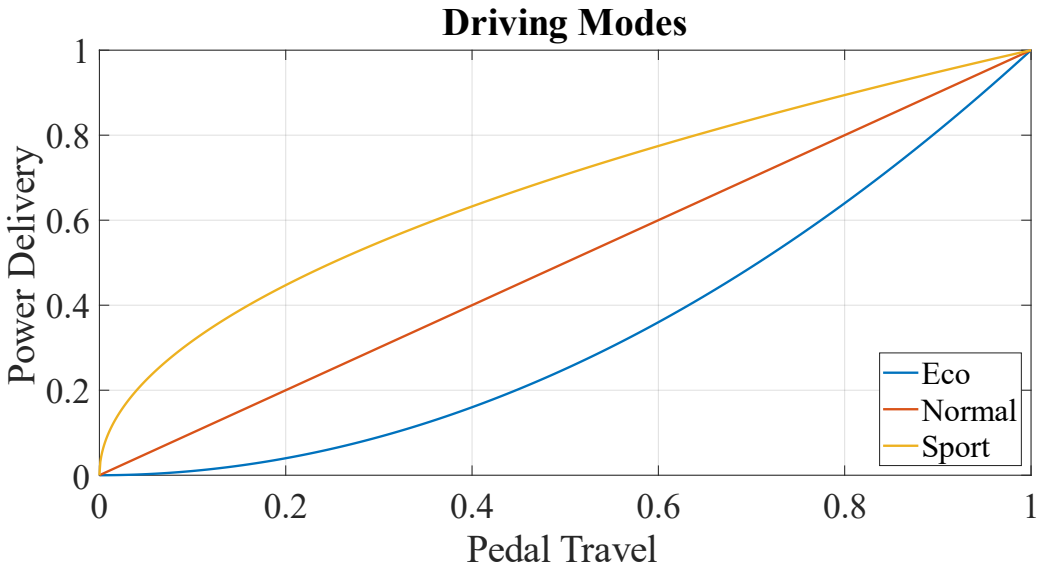

Fig. 1. Commercially available driving modes in performance cars and above

energy economy in the EVs, the eco-driving problem is studied and optimised here. Beneficially, the improved energy economy also translates into an extended range of the EVs, a major anxiety among the EV owners [7], [8]. Hence, studying eco-driving systems to further the benefits and make transport more sustainable is relevant.

Eco-mode available in on-road vehicles achieves several tasks. Of these, modifying driver inputs is one of the technological ways of improving the energy economy that does not require any structural changes to the system. Driver inputs can be modified by controlling the powertrain response, or by directly providing feedback and feedforward advice to the driver based on the past and the current driving performances respectively for him/her to adopt an energy-aware driving style [1]. The latter translates into the driver following an energy-optimal speed trajectory advised by the eco-driving system. The trajectory minimises losses such as those due to the aerodynamic drag and the dissipative braking during downhill driving [9]. Van Keulen and Salazar [10] computed the optimal speed trajectory for a hybrid electric vehicle to generate energy-aware driving advice for a straight line manoeuvre with near-halt beginning and ending conditions. This thesis is an extended adaptation of their work to an EV.

1.2 Research Objective

First, the present solution methods for eco-driving problems lack sufficient generality to optimise the speed trajectories for vehicles for various loading conditions and when they travel a wide range of distances. And second, the optimisation of trajectories for EVs driving on graded roads has not yet been performed to our best knowledge. These two research gaps, in theory, limit the applicability of eco-driving systems for EVs thereby limiting their operational efficiency.

In this thesis, we propose a new solution method to compute the energy-optimal speed trajectories that is robust to the loading conditions, the distance the vehicle must cover and the road profile it travels on. In the end, we test the global optimality of the speed trajectories by convexification of the problem and then solving it to compute the globally optimal speed trajectory.

We limit the scope of this thesis to testing the robustness and the global optimality of the proposed numerical solution in simulation. In practice, it can be extended to training the drivers on driving simulators for them inculcate energy-aware driving behaviour. They would achieve this by following the advised optimal speed trajectories and then practising the behaviour on on-road EVs to minimise energy consumption.

1.3 Thesis Outline

The remainder of the thesis is structured as follows: Chapter 2 mathematically states the eco-driving problem for EVs that we solve by optimising the speed trajectories and describes the electric powertrain architecture for which we state the problem. In chapter 3, we reformulate the problem into a two-point boundary value problem whose dynamics are governed by a coupled system of ODEs subject to boundary conditions. In addition, we propose the solution method. We present and interpret the results of the simulations for different vehicle parameters and driving conditions in chapter 4. In chapter 5, we perform convexification of the problem and solve it to compute the globally optimal speed trajectory for the first result in chapter 4, to test the global optimality of the proposed solution. Finally, chapter 6 summarises the work done and suggests potential extensions.

2

Electric Powertrain Architecture and Problem Definition

To propel forward, a BEV efficiently utilises the stored electrical energy E_s (refer Fig. 2) in its battery pack, to power the electric motors on which the vehicle solely runs. Before the power P_s is transmitted to the motors via the motor controllers, it suffers from electrical resistance losses within the battery. Note that the same resistance also limits the regeneration of E_s from incoming power from the motors during deceleration. Finally, the motor consumes the power P_b to provide mechanical power P_m to achieve the desired kinetic energy of the vehicle E_k.

During forward propulsion, the vehicle suffers from 3 losses primarily:

1. Rolling resistance of the tires
2. Aerodynamic drag, and
3. Gravitational pull (push) in case of positively (negatively) graded roads.

We represent the algebraic sum of the 3 losses as P_l. While braking, when the required brake power exceeds the maximum braking the motors can provide while regenerating, the driver applies mechanical brakes. This mechanical brake power is P_d and is null during forward propulsion. Lastly, the cumulative power available to cause the desired change in the kinetic energy of the vehicle is P_r.

The aim of eco-driving system is to minimise the expenditure of E_s for any given trip. Mathematically, the eco-driving optimal control problem becomes

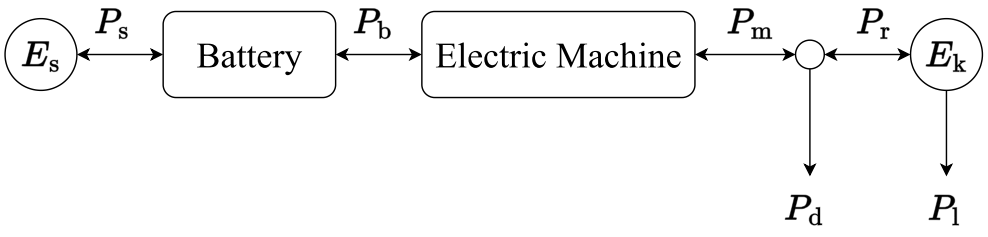

Fig. 2. Powertrain Architecture of a BEV

Table 1. Summary of Parameters of the Powertrain Architecture of a BEV

Name	Description
E_s	Stored electrical energy
P_b	Rate of consumption of electrical energy after electrical resistance losses during acceleration or regeneration before electrical resistance losses during deceleration
P_s	Rate of consumption of electrical energy before electrical resistance losses during acceleration or regeneration after electrical resistance losses during deceleration
P_m	Power delivered by ($P_\mathrm{m} > 0$)/ to ($P_\mathrm{m} < 0$) electric motor
P_r	Power delivered to provide the required increase in kinetic energy ($P_\mathrm{r} > 0$) or recovered from its decrease ($P_\mathrm{r} < 0$)
E_k	Kinetic energy of the BEV
P_d	Mechanical brake power consumed during deceleration
P_l	Power loss due to rolling resistance, aerodynamic drag and gravity

$$\begin{aligned} \min_{P_\mathrm{m},P_\mathrm{d}} \quad & \int_0^T P_\mathrm{s}\,\mathrm{d}t \\ \text{s.t.} \quad & \dot{E}_\mathrm{k}(t) = P_\mathrm{m}(t) - P_\mathrm{d}(t) - P_\mathrm{l}(t) \\ & \dot{s}(t) = \sqrt{\frac{2}{m}\cdot E_\mathrm{k}(t)} \\ \text{and} \quad & E_\mathrm{k}(t=0) = E_\mathrm{k,o} \\ & E_\mathrm{k}(t=T) = E_\mathrm{k,f} \\ & s(t=0) = 0 \\ & s(t=T) = s_\mathrm{f}, \end{aligned} \tag{1}$$

where s_f is the distance the vehicle of mass m covers in time T. The initial and the final kinetic energy of the vehicle are $E_\mathrm{k,o}$ and $E_\mathrm{k,f}$ respectively. Hence, we apply the boundary conditions on the initial and the final states of the distance covered and the kinetic energy. The vehicle suffers from the power loss P_l due to the rolling resistance, the aerodynamic drag and the gravity. The driver controls the power flow to/ from the electric motor P_m as well as the mechanical brake power P_d through the accelerator and the brake pedals respectively. The electric motor power flow P_m causes the battery state of energy E_s to vary as per $\dot{E}_\mathrm{s} = -P_\mathrm{s}(P_\mathrm{m})$, where

$$P_\mathrm{s} = \frac{U_\mathrm{o}}{2\cdot R}\cdot\left(U_\mathrm{o} - \sqrt{U_\mathrm{o}^2 - 4\cdot R\cdot\frac{1}{{\eta_\mathrm{m}}^{\mathrm{sgn}(P_\mathrm{m})}}\cdot P_\mathrm{m}}\right), \tag{2}$$

for a null voltage increase factor, discharged battery voltage U_o, internal resistance of the battery R and the electric motor efficiency η_m [10].

In this thesis, we solve the problem (1) describes for manoeuvres that generate the same results as those of straight line driving, i.e. the cornering radii on the road are significantly large to render the lateral dynamics of the vehicle negligible.

To prove the robustness of the proposed solution method against different vehicle parameters and driving conditions, the above problem is first solved for the specifications of an EV, and then for the increasing:

1. Loading conditions of the vehicle
2. Distances to be covered, and
3. Road grade.

In addition to constant road grades, the proposed solution method also solves the problem for variable road grade to capture the interesting ways in which the eco-driving system exploits gravitationally assisted propulsion.

The following chapter formally derives the coupled system of ODEs and proposes the solution method to generate the optimal speed trajectories by solving the system.

3

Problem Reformulation and Solution Method

To generate the optimal speed trajectories by solving the problem in (1), two commonly used optimal control methods in literature make to the list of choices. These are Dynamic Programming (DP) and Pontryagin's Minimum Principle (PMP). DP is a numerical method to generate globally optimal solutions of optimisation problems. Advantageously, it provides optimal results for non-smooth and non-linear cost functions and constraints [11]. This method has been used to solve various problems in eco-driving. For example, Hellström et al. [12] employed this method to optimise velocity profile and gear shift strategy, and chose Euler forward method of discretisation to minimise quantisation errors. Kamalanathsharma and Rakha [13] again achieved optimal velocity profile but then proposed multi-stage DP to show its computational efficiency.

However, DP suffers from two main drawbacks: the quantisation errors and the increasingly required processing power as the number of variables increases. To mitigate these limitations, certain simplifications to the model have been performed by some researchers. For example, to ease the curse of dimensionality, discrete DP with forward recursion was implemented without having time as a state variable to generate quasi-global-optimum results [14]. Nevertheless, such modifications cannot always be made. On the other hand, PMP provides analytical conditions that allows to rewrite an optimal control problem into a two-point Hamiltonian boundary value problem (BVP). It does not suffer from discretisation errors before solution and is efficient at handling larger systems. Hence, for the problem (1) describes, it is convenient and computationally efficient to employ PMP. It, however, does not guarantee global optimality for non-convex problems, or in absence of a unique solution, its optimality must be verified. In chapter 5, this is achieved by convexification of the problem.

Van Keulen and Salazar [10] leverage PMP to derive the optimal energy management policy for an HEV jointly for a fixed distance and time. A similar approach is used here to translate (1) optimal control problem into a system of ODEs with initial conditions by applying PMP. The solution of the system is void of any rapidly varying nearby solutions. Hence, the system is non-stiff thereby making the `ode45` algorithm of Matlab appropriate for the solution.

3.1 Application of PMP to Generate Two Point BVP

Here, we derive the system of ODEs described for (1). Application of PMP (see Appendix) transforms the global optimization problem (1) into an instantaneous Hamiltonian optimization problem [15]. Thus, to optimise the problem, we minimise the instantaneous Hamiltonian H defined as

$$H = P_{\mathrm{s}} + \begin{bmatrix} -\lambda_{\mathrm{k}} \\ -\lambda_{\mathrm{s}} \end{bmatrix}^{T} \cdot \begin{bmatrix} \dot{E}_{\mathrm{k}} \\ \dot{s} \end{bmatrix} = \lambda_{\mathrm{k}} \cdot (P_{\mathrm{d}} + P_{\mathrm{l}} - P_{\mathrm{m}}) - \lambda_{\mathrm{s}} \cdot v + P_{\mathrm{s}}. \tag{3}$$

We derive the time derivatives of the two state variables E_{k} and s from the powertrain architecture in Fig. 2. Subsequently, computing the state dynamics from Fig. 1 and the co-state dynamics using (3), the resultant system of ODEs is

$$\begin{bmatrix} \dot{E}_{\mathrm{k}} \\ \dot{s} \\ \dot{\lambda}_{\mathrm{k}} \\ \dot{\lambda}_{\mathrm{s}} \end{bmatrix} = \begin{bmatrix} P_{\mathrm{m}} - P_{\mathrm{d}} - P_{\mathrm{l}} \\ v \\ \dfrac{\partial H}{\partial E_{\mathrm{k}}} \\ \dfrac{\partial H}{\partial s} \end{bmatrix} \tag{4}$$

$With\ boundary\ conditions$:
$E_{\mathrm{k}}(t = 0) = E_{\mathrm{k,o}}$
$E_{\mathrm{k}}(t = T) = E_{\mathrm{k,f}}$
$s(t = 0) = 0$
$s(t = T) = s_{\mathrm{f}}$.

The co-state variables, λ_{k} and λ_{s} quantify the cost of moving the corresponding state variables from their optimal positions. For positive co-state variables, the higher the magnitude of the co-state variables, the more favourable for the objective function it becomes to increase the magnitude of the corresponding state variable. For the sake of simplicity, the instantaneous velocity v is used interchangeably with the quantity $\sqrt{\frac{2}{m} \cdot E_{\mathrm{k}}}$. The remaining required vehicle parameters are summarised in Table 2.

To derive the optimal power delivered by/ to the electric motor, we equate the derivative of the Hamiltonian with respect to the motor power to 0 followed by constraining the motor power with its peak positive and negative power, i.e.

Table 2. Summary of the Vehicle Parameters

Name	Description
η_{m}	Electric motor efficiency
$\bar{P}_{\mathrm{m}}$	Peak power of the electric motor
$\underline{P}_{\mathrm{m}}$	Negative peak power of the electric motor
U_{o}	Discharged battery voltage
R	Internal resistance of the battery
m	Curb weight of the vehicle
c_{r}	Rolling resistance coefficient
c_{d}	Aerodynamic drag coefficient
A	Frontal area of the vehicle
ρ	Density of the ambient air
g	Gravitational constant
$\bar{P}_{\mathrm{d}}$	Maximum brake power

$$\frac{\partial H}{\partial P_{\mathrm{m}}} = 0 \Rightarrow \frac{\partial P_{\mathrm{s}}}{\partial P_{\mathrm{m}}} - \lambda_{\mathrm{k}} = 0$$
$$\Rightarrow \lambda_{\mathrm{k}} = \frac{U_{\mathrm{o}}}{{\eta_{\mathrm{m}}}^{\mathrm{sgn}(P_{\mathrm{m}})} \cdot \sqrt{U_{\mathrm{o}}^2 - 4 \cdot R \cdot \frac{1}{{\eta_{\mathrm{m}}}^{\mathrm{sgn}(P_{\mathrm{m}})}} \cdot P_{\mathrm{m}}}}. \tag{5}$$

Rearranging the terms,

$$P_{\mathrm{m}} = \begin{cases} \frac{{U_{\mathrm{o}}}^2}{4 \cdot R \cdot \eta_{\mathrm{m}}} \cdot \left(1 - \frac{{\eta_{\mathrm{m}}}^2}{{\lambda_{\mathrm{k}}}^2}\right) & \lambda_{\mathrm{k}} < \eta_{\mathrm{m}} \\ 0 & \eta_{\mathrm{m}} \le \lambda_{\mathrm{k}} \le \frac{1}{\eta_{\mathrm{m}}} \\ \frac{{U_{\mathrm{o}}}^2 \cdot \eta_{\mathrm{m}}}{4 \cdot R} \cdot \left(1 - \frac{1}{{\eta_{\mathrm{m}}}^2 \cdot {\lambda_{\mathrm{k}}}^2}\right) & \frac{1}{\eta_{\mathrm{m}}} < \lambda_{\mathrm{k}}. \end{cases} \tag{6}$$

To limit (6) with the peak motor power such that $P_{\mathrm{m}} \in \left[\underline{P}_{\mathrm{m}}, \bar{P}_{\mathrm{m}}\right]$, the motor power

$$P_{\mathrm{m}} = \begin{cases} \max\left[\underline{P}_{\mathrm{m}}, \frac{{U_{\mathrm{o}}}^2}{4 \cdot R \cdot \eta_{\mathrm{m}}} \cdot \left(1 - \frac{{\eta_{\mathrm{m}}}^2}{{\lambda_{\mathrm{k}}}^2}\right)\right] & \lambda_{\mathrm{k}} < \eta_{\mathrm{m}} \\ 0 & \eta_{\mathrm{m}} \le \lambda_{\mathrm{k}} \le \frac{1}{\eta_{\mathrm{m}}} \\ \min\left[\bar{P}_{\mathrm{m}}, \frac{{U_{\mathrm{o}}}^2 \cdot \eta_{\mathrm{m}}}{4 \cdot R} \cdot \left(1 - \frac{1}{{\eta_{\mathrm{m}}}^2 \cdot {\lambda_{\mathrm{k}}}^2}\right)\right] & \frac{1}{\eta_{\mathrm{m}}} < \lambda_{\mathrm{k}}. \end{cases} \tag{7}$$

To derive the optimal mechanical brake power P_{d}, we minimise the Hamiltonian with respect to P_{d}. The Hamiltonian is affine in it and the non-triviality condition, i.e. no solutions lie outside the general solution, eliminates a singular solution in $\left[0, \overline{P}_{\mathrm{d}}\right]$. Therefore, the optimal mechanical brake power is

$$P_{\mathrm{d}} = \begin{cases} 0 & \lambda_{\mathrm{k}} \geq 0 \\ \overline{P}_{\mathrm{d}} & \lambda_{\mathrm{k}} < 0. \end{cases} \tag{8}$$

Apart from the driver inputs P_{m} and P_{d}, the external power loss P_{l} directly influences the rate of change of E_{k}. This power loss is the algebraic sum of the rolling resistance, the aerodynamic drag and the gravitational push/ pull, and equals

$$P_{\mathrm{l}} = c_{\mathrm{r}} \cdot m \cdot g \cdot v \cdot \cos\theta + \frac{1}{2} \cdot \rho \cdot A \cdot c_{\mathrm{d}} \cdot v^3 + m \cdot g \cdot v \cdot \sin\theta, \tag{9}$$

for the road grade $\theta = \theta(s)$. We now derive the dynamics of the co-state variables. From (3), the Hamiltonian depends on the state variable s through the road grade. For a maximum road grade of x %, let the equivalent angle in radians be θ_{amp}. Then

$$\theta_{\mathrm{amp}} = \tan^{-1}\left(\frac{x}{100}\right). \tag{10}$$

In order that one sine period spans the driving distance, the frequency of the wave becomes

$$\omega = \frac{2 \cdot \pi}{s_{\mathrm{f}}}. \tag{11}$$

This leads to the instantaneous road grade θ in radians as a function of distance travelled s to be

$$\theta = \theta_{\mathrm{amp}} \cdot \sin(\omega \cdot s). \tag{12}$$

We substitute (14) in (10) to derive the distance co-state dynamics $\dot{\lambda}_{\mathrm{s}}$ by taking the space derivative of Hamiltonian in (3) as

$$\begin{aligned}\dot{\lambda}_{\mathrm{s}} &= \frac{\partial H}{\partial s} \\ &= \lambda_{\mathrm{k}} \cdot \frac{\partial P_{\mathrm{l}}}{\partial s} \\ &= \lambda_{\mathrm{k}} \cdot \left(-c_{\mathrm{r}} \cdot m \cdot g \cdot v \cdot \sin\theta(s) \cdot \frac{\partial \theta(s)}{\partial s} + m \cdot g \cdot v \cdot \cos\theta(s) \cdot \frac{\partial \theta(s)}{\partial s} \right) \\ &= \lambda_{\mathrm{k}} \cdot m \cdot g \cdot v \cdot \theta_{\mathrm{amp}} \cdot \omega \cdot \cos(\omega \cdot s) \cdot (\cos\theta(s) - c_{\mathrm{r}} \cdot \sin\theta(s)).\end{aligned} \tag{13}$$

Finally, the kinetic energy co-state dynamics equal

$$\begin{aligned}\dot{\lambda}_{\mathrm{k}} &= \frac{\partial H}{\partial E_{\mathrm{k}}} \\ &= \lambda_{\mathrm{k}} \cdot \frac{\partial P_{\mathrm{l}}}{\partial v} \cdot \frac{\partial v}{\partial E_{\mathrm{k}}} - \lambda_{\mathrm{s}} \cdot \frac{\partial v}{\partial E_{\mathrm{k}}} \\ &= \lambda_{\mathrm{k}} \cdot \left(\frac{c_{\mathrm{r}} \cdot g \cdot \cos\theta + g \cdot \sin\theta}{v} + \frac{3 \cdot \rho \cdot A \cdot c_{\mathrm{d}} . v}{2 \cdot m} \right) - \frac{\lambda_{\mathrm{s}}}{m \cdot v}.\end{aligned} \tag{14}$$

Dib et al. [16] employ the same tool for a BEV and show the equivalency between finding the optimal speed trajectory and problem of solving a system of two algebraic equations. Incorporation of gear shifting strategy to switch the state dynamics in BVP formed by PMP as done in [17] is not performed here.

3.2 Solution Method

We cannot integrate the system of ODEs in (4) subject to (7)–(9), (13) and (14) as an initial value problem because the boundary conditions of the distance and the velocity are defined at final time also while we cannot derive the initial values of the co-states analytically. However, the system is closed because 4 conditions are provided for 4 coupled differential equations.

By iterating the initial values of the co-states for fixed initial values of the states, we find the initial values of the co-states that lead to the final state values coinciding with their terminal conditions. For a fixed initial small guess of λ_{k}, the final velocity varies inversely with increasing initial small guess of λ_{s}. And for each set of $\lambda_{\mathrm{k}}(t = 0)$ and $\lambda_{\mathrm{s}}(t = 0)$ satisfying the final kinetic energy condition, the distance the vehicle covers increases monotonically with increasing $\lambda_{\mathrm{k}}(t = 0)$. Hence, both λ_{k} and λ_{s} are iterated with the positive variable co-state increments $\Delta\lambda_{\mathrm{k}}$ and $\Delta\lambda_{\mathrm{s}}$ respectively as per the decision tree in Fig. 3 until we arrive at the unique solution that satisfies both the initial and the final state boundary conditions. Each time the final kinetic energy decreases below, or/ and the distance covered increases above the respective terminal conditions, the initial value of the corresponding co-state is restored to its previous value and the corresponding increment decreases by the order of 10. The loop terminates when either all the boundary conditions are met or when the increments decrease below the default precision of Matlab. We follow this methodology to optimise the speed trajectories and present the results in chapter 4.

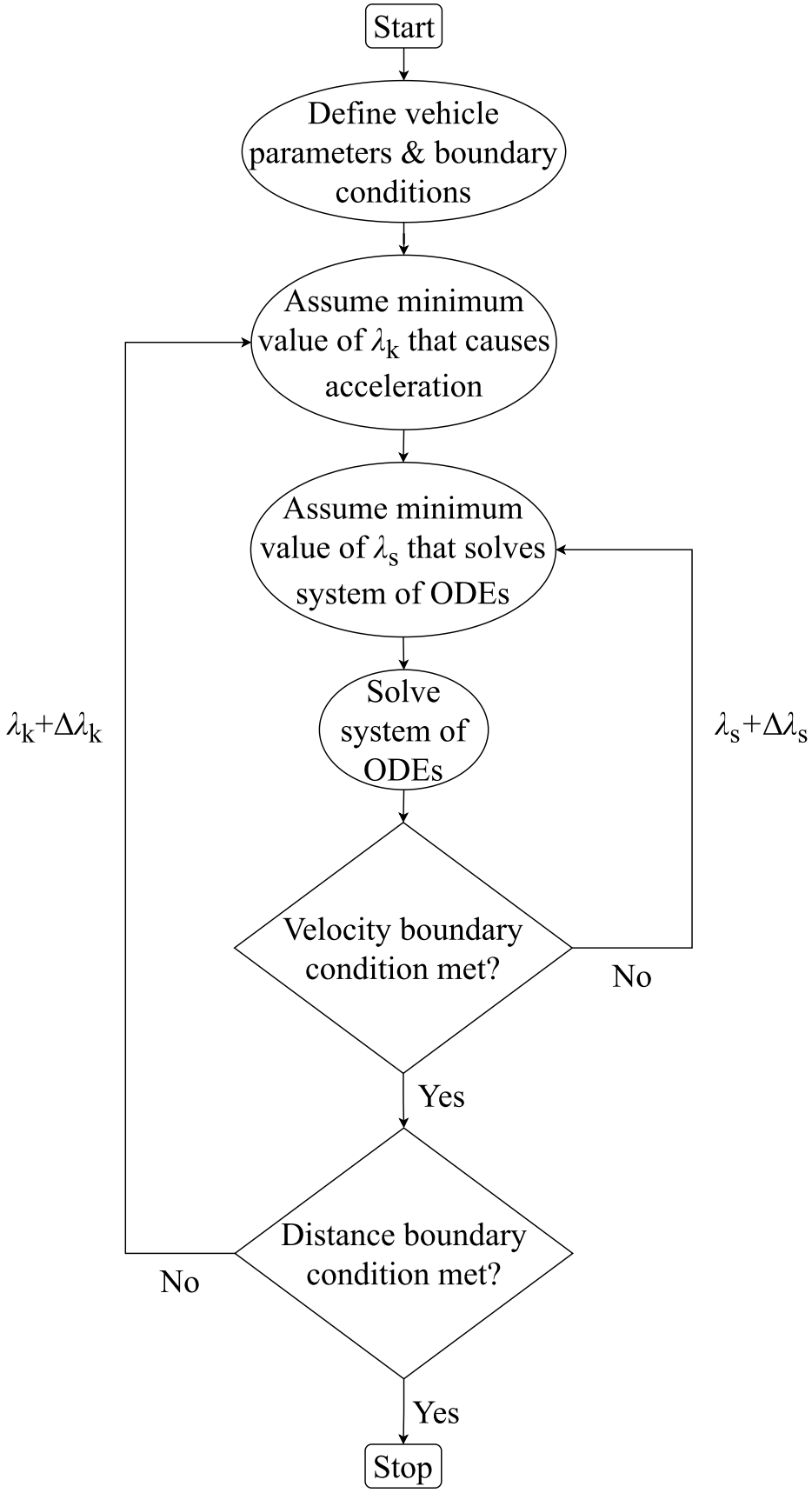

Fig. 3. Decision tree for optimisation of the speed trajectories for the eco-driving system

4

Optimisation Results

In this chapter, we solve the system of ODEs described by (4) subject to (7)–(11) for an EV driving a near-straight distance of $s = 6\text{km}$ in travel time $T = 200\text{s}$ on a flat road followed by solutions for varying loading conditions of the vehicle, distances to be covered and road grades. This driving manoeuvre is representative of one of the simplest manoeuvres into which longer and more complex speed trajectories can be divided. Thus, we optimise the speed trajectory for one of its sections. We can extend this approach to the remaining sections of the speed trajectory when there exist speed waypoints. Sequentially concatenating the section-wise optimal speed trajectories to form the entire speed trajectory produces the same speed trajectory as by optimising the entire speed trajectory with waypoints at once, given the Bellman's Principle of Optimality [18].

We use the vehicle specifications in Table 3 to simulate the near-straight line driving manoeuvre. For the remainder of the thesis, we assume the vehicle to be fully charged in the beginning with the initial battery state of energy $E_{\text{s,o}} = 306\text{MJ}$ for all cases.

The following two assumptions are made to iterate the initial values of the co-states more informatively:

1. Minimum velocity of the vehicle is $1 \pm 0.5\ \text{m/s}$ to maintain $\dot{\lambda}_{\text{k}}$ real, i.e. the vehicle is never at complete standstill to prevent λ_{k} from exploding (see (11)). The margin of $\pm 0.5\ \text{m/s}$ is introduced to avoid requiring a precision greater than the 16 digits precision (double precision) which Matlab uses by default.

Table 3. Vehicle Parameter Values

Name	Value	Units
η_{m}	0.9	–
$\bar{P}_{\text{m}}$	310	kW
$\underline{P}_{\text{m}}$	-310	kW
U_{o}	346	V
R	0.32	Ω
m	2108	kg
c_{r}	0.01	–
c_{d}	0.24	–
A	2.34	m^2
ρ	1.2	kg/m^3
g	9.81	m/s^2
$\bar{P}_{\text{d}}$	20	kW

2. The vehicle always accelerates at $t = 0$ s. This allows to guess the initial value of $\lambda_{\mathrm{k}} = \frac{1}{\eta_{\mathrm{m}}} + \delta$ where δ is the smallest positive value for which the state space dynamics is real for the entire trip duration $t \in [0, T]$. From observation, the least value of δ corresponds to the least final distance s_{f} the vehicle must cover for the eco-driving system to result in sufficient electrical energy savings.

The original case for which we solve the problem now is when a regularly loaded EV covers 6km distance within 200s on flat road. Fig. 4 shows the optimal speed trajectory and the variation of the battery state of energy for this case, and Fig. 5 shows the driver inputs that achieve the optimal speed trajectory.

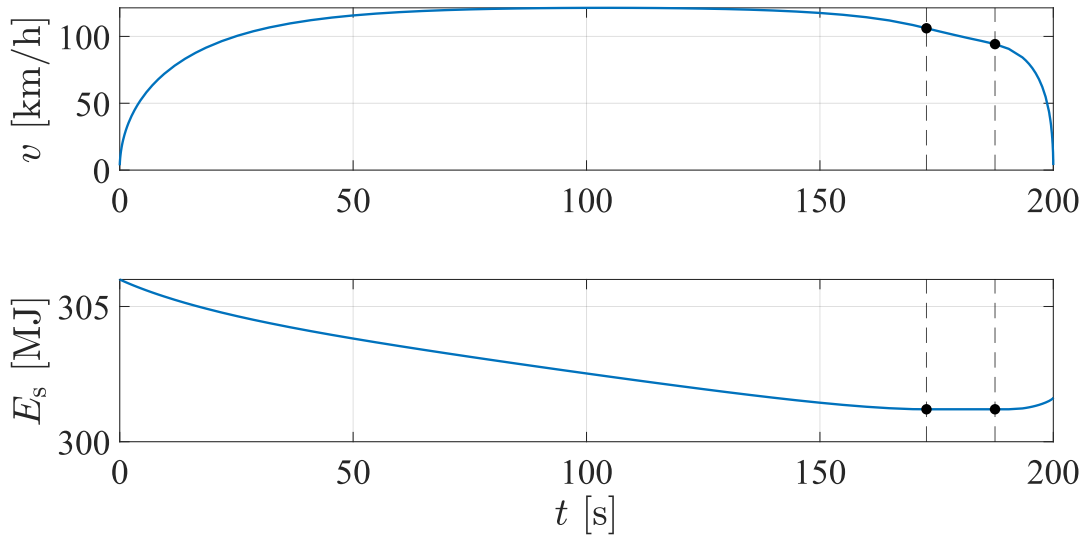

Fig. 4. Energy-optimal speed and battery state of energy trajectories of a regularly loaded BEV on a flat road

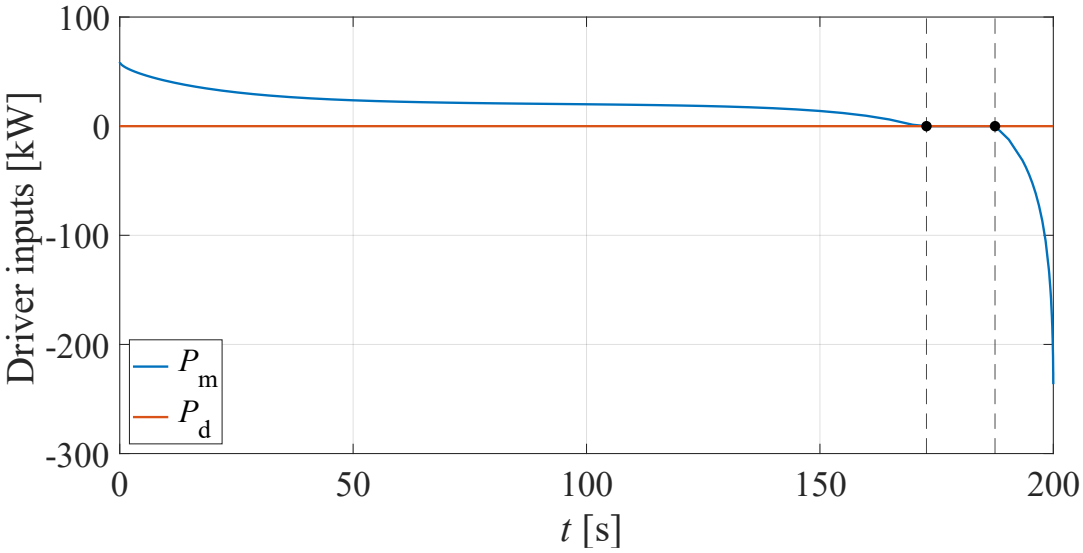

Fig. 5. Variation of driver inputs for a regularly loaded BEV on a flat road

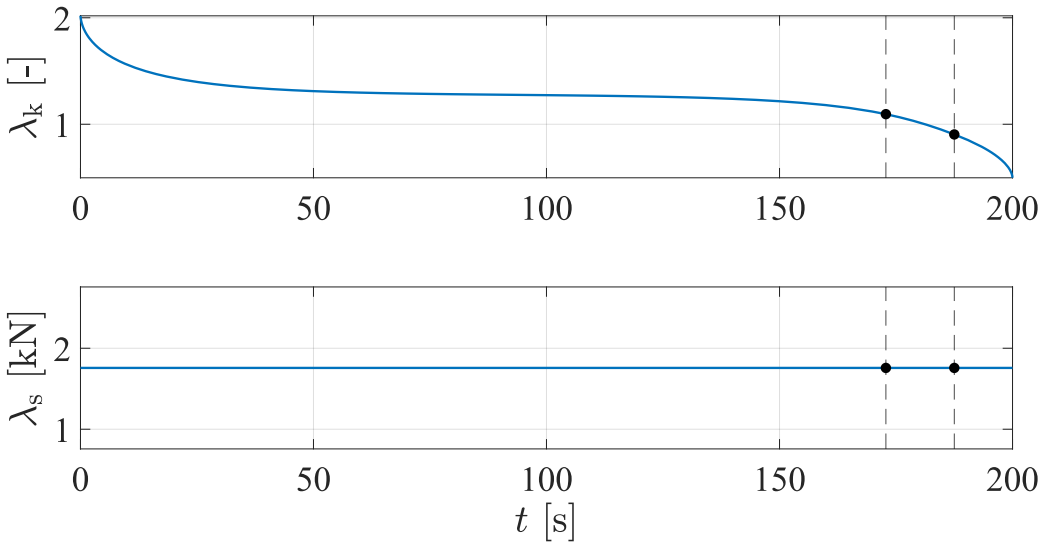

Fig. 6. Optimal co-state trajectories of a regularly loaded BEV on a flat road

The velocity trajectory shows that to minimise the net consumption of electrical energy, it is optimal for the vehicle to accelerate for more than half of the trip duration. It starts with steep acceleration to attain the near-cruising velocity followed by a significantly gradual acceleration. Note that the vehicle continues to draw power during the cruising phase because it continuously suffers from the power loss P_l. As the vehicle begins to decelerate, the rate of change of battery state of energy first stagnates, as depicted by the region between the two dashed lines to represent the costing phase, and then increases due to regeneration. Following the coasting phase, the power loss P_l acts in the favour of the desired rate of change of E_k. Consequently, the deceleration phase is significantly shorter and steeper than the acceleration phase wherein the resistances oppose the desired motion of vehicle unlike during the deceleration phase. Steeper deceleration phase rapidly regenerates a portion of the spent electrical energy but the short duration over which this occurs limits the quantity of the regenerated energy per se.

The time period between the two vertical dashed lines denotes the duration following the cruising phase when the rolling resistance and aerodynamic drag, the gravitational load being zero for flat roads, alone decelerate the vehicle. Here, the electric motor neither consumes nor provides power. It is only after this phase that the kinetic energy co-state λ_k reduces below the electric motor efficiency thereby driving the motor to work as a generator as per (11). Fig. 6 shows the co-evolution of λ_k with λ_s with respect to time. The higher the value of λ_k, the more beneficial it becomes from the energy point of view to increase the velocity of the vehicle and vice-versa. The evolution of λ_s is however constant as the Hamiltonian is independent of the distance state s for flat roads.

We interpreted the energy-optimal state and co-state trajectories to correlate their evolutions with the expected physical motion of the EV. This improves understanding of the speed trajectories that the eco-driving system generates to promote energy-aware driving behaviour.

Next, these trajectories vary subject to vehicle parameters and driving conditions. Because the proposed solution method is independent of the vehicle mass, the distance to be covered and the road grade, we now use it to optimise the speed trajectories for the case when the vehicle:

1. Is heavily loaded
2. Drives longer distances
3. Must traverse graded roads

4.1 Loaded Vehicle

The vehicle specifications provided by the vehicle only state the curb weight which excludes the weight of passengers and cargo. The latter weight varies from one trip to another and so does the energy-optimal speed trajectory. Here, the combined added weight of up to

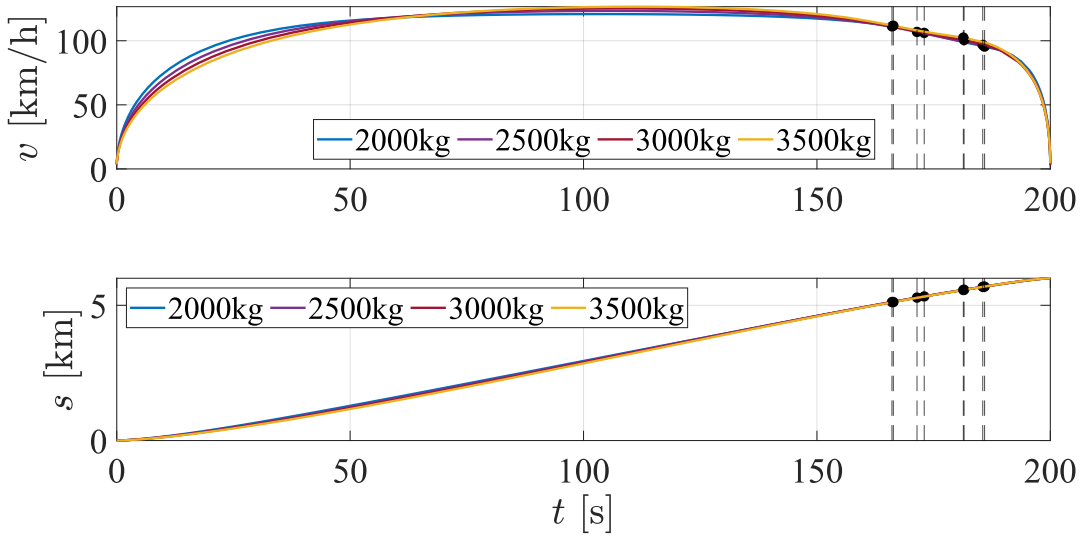

Fig. 7. Energy-optimal state trajectories for increasing vehicle mass on a flat road

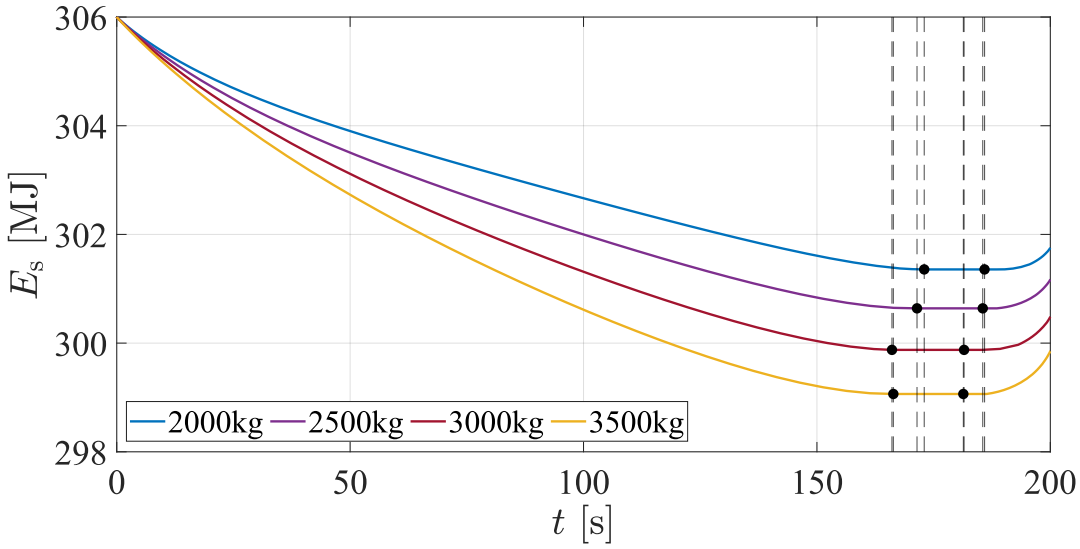

Fig. 8. Variation of battery state of energy for increasing vehicle mass on a flat road

approximately 1500kg is considered to analyse and interpret the variations in optimal speed trajectories.

A direct consequence of the increasing vehicle mass is its increased inertia which demands greater input and output power from the electric motor. To maintain a smoother ride, the vehicle now spends longer to accelerate and decelerate (Fig. 7) instead of maintaining the same duration of cruising phase which would require more aggressive acceleration and deceleration. Consequently, to reach the destination timely, the vehicle maintains a higher peak velocity that compensates for the otherwise decrease in distance covered due to shorter cruising phase.

A loaded vehicle suffers from a greater rolling resistance, the gravitational load and the inertia. The gravitational load is absent here because the road is not yet graded. Increased rolling resistance causes the motor to consume stored energy at a greater rate. This is seen from Fig. 8. Both longer and more aggressive deceleration mean that a higher amount of energy is regenerated. However, the net consumption remains higher for a loaded vehicle. In conclusion, it is optimal from the energy point of view for a loaded vehicle to accelerate and decelerate slower to achieve a higher peak velocity for a shorter duration to traverse the desired distance timely, beginning and ending with near halt condition.

4.2 Longer Distances

For the vehicle to travel farther with available time being constant, we observe that the cruising phase shortens. Shortened cruising phase increases the peak velocity and maintains a higher velocity throughout the trip to complete it timely. Here, the ride comfort is compromised due to increasingly aggressive accelerations and decelerations evident from the velocity trajectories. Although the eco-driving system generates optimal speed trajectories, it does not account for their feasibility. For instance, driving over 150 km/h on busy urban roads may not be reachable. Clearly, additional constraints on the maximum velocity and, peak acceleration and deceleration are desirable. For the sake of simplicity, we neglect these constraints here.

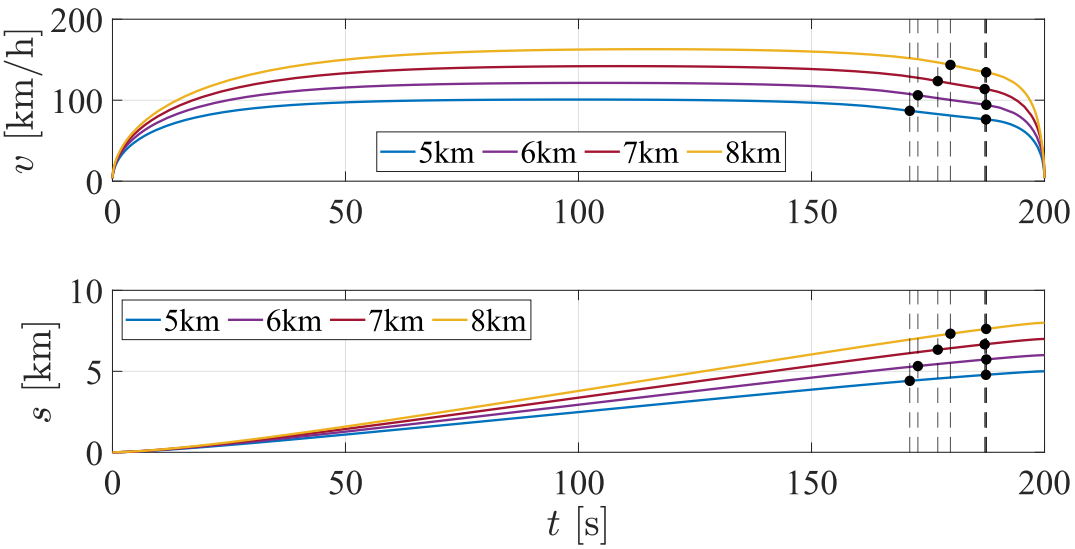

Fig. 9. Energy-optimal state trajectories of a regularly loaded BEV covering longer distances on a flat road

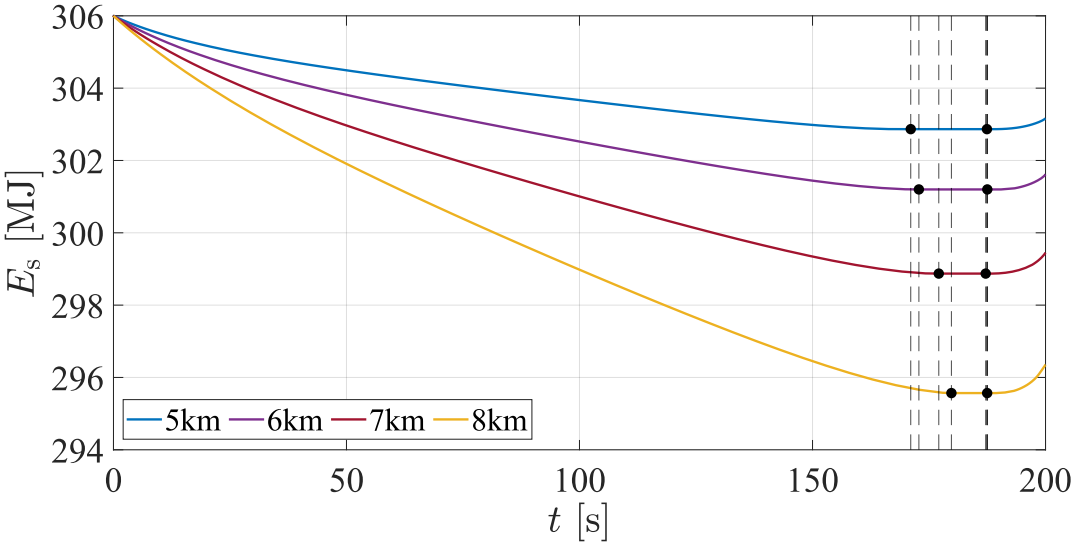

Fig. 10. Variation of battery state of energy of a regularly loaded BEV covering longer distances on a flat road

The energy aware driving approach here becomes: accelerate and decelerate harder to achieve a higher peak velocity for a shorter duration to traverse longer distances timely and minimise net the consumption of energy. The following section shows the influence on speed trajectories by one of the topographical features of roads: road grade.

4.3 Driving on Graded Roads

Observed road grades in the environment are often less than 10%. However, they can significantly increase the consumption of stored energy and hence, must not be neglected [19]. While a positive road gradient leads to increased tendency of driver to accelerate thereby consuming greater energy [19]–[21], a negative road grade allows for a more conservative expenditure of stored electrical energy due to gravitationally assisted propulsion. Clearly, the road grade influences the power loss term P_l illustrated in Fig. 2. By optimising the velocity trajectories for various power loss, eco-driving system again reduces energy consumption on graded roads specifically where the drivers unknowingly cause their vehicles to consume more energy than necessary. This section studies the impact of both constant and variable road grades on optimal speed trajectories.

4.3.1 Constant Road Grade

Here, the driving manoeuvre described in the problem definition is simulated on positively graded roads up to 9%.

The first observation is that driving uphill negatively impacts the initial acceleration due to increased gravitational load. Here, eco-driving suggests a slightly harder acceleration to reach the cruising velocity earlier than in the case of flat roads. Consequently, longer cruising phase minimises the maximum velocity the vehicle must attain to reach the destination timely. Both longer cruising phase and minimum peak velocity increasingly shorten the duration of deceleration phase, as observed from the velocity trajectories in Fig. 11, at the end of which the vehicle is to come to a near halt. This also implies that the quantity of regenerated energy

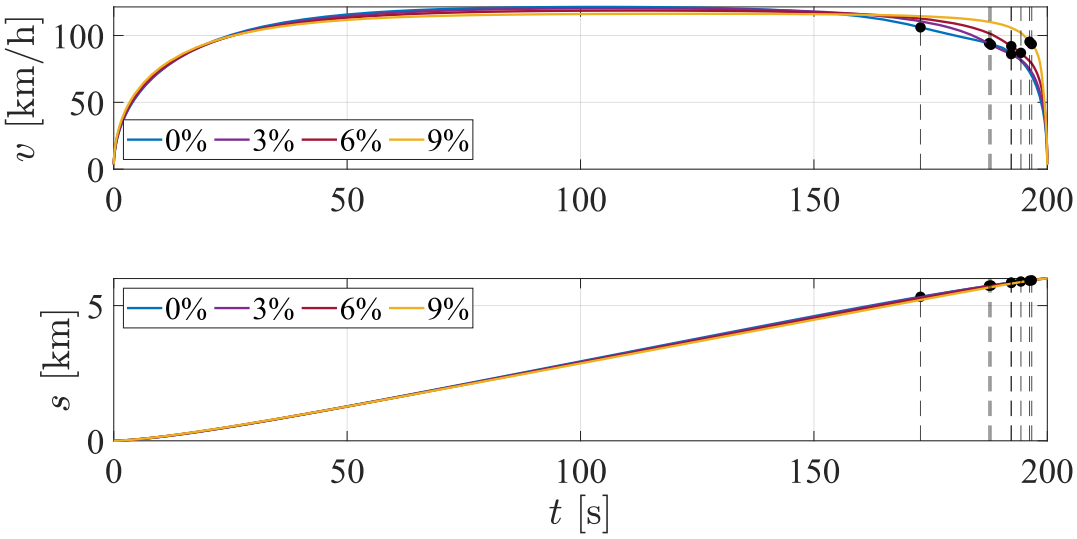

Fig. 11. Energy-optimal speed and distance trajectories for increasing road grades

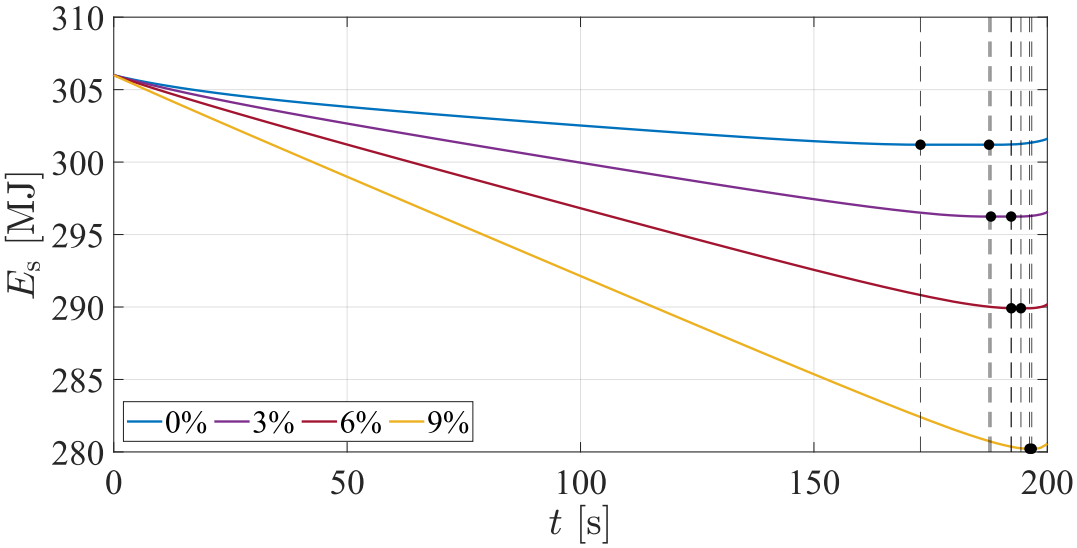

Fig. 12. Variation of battery state of energy for increasing road grades

is reduced even though the rate of regeneration is higher due to more aggressive deceleration. It can be calculated from the plot in Fig. 12 that for the same distance to be covered, time available being constant, more aggressive deceleration for shorter time period results in lesser net amount of energy generated compared to that on flat roads where the deceleration rate is lower but duration is more.

According to eco-driving system, in order to minimise the net amount of energy consumed during the entire trip, it is desirable to quickly begin cruising at a lower velocity by accelerating more aggressively followed by braking harder to come to the near halt. This is counterintuitive as such acceleration and deceleration behaviours are mistakenly understood to oppose the smoother driving behaviours that eco-driving aims to maintain on flat roads. However, it must be noted that the acceleration and deceleration behaviours that eco-driving advise here are yet smoother than the ones observed in driving the same path without the eco-driving system.

4.3.2 Variable Road Grade

Due to Earth's diverse topography, the inclination of roads varies from one region to another. Hence, for sufficiently large distances, incorporating continuously varying road grades into the problem description yields greater energy savings than those yielded by eco-driving systems neglecting the local road grade. To capture the effect of varying road grades over large distances, the distance of 6 km modelled so far now comprises of varying road grade as per a sine wave.

For the road grade amplitude of $\theta_{\text{amp}} = 1\%$, the road grade and altitude vary as in Fig. 13. The solution of the system of ODEs in (4) now subject to (7)–(9), (13) and (14) following the same decision tree in Fig. 3 yields the optimal speed trajectory.

Again, the vehicle first accelerates to achieve the cruising phase quickly. As the road begins to decline, the vehicle propulsion is gravitationally assisted, consumption of the stored energy stagnates as indicated in the region between the two dashed lines, the vehicle leverages its momentum to coast and begins to regenerate a portion of its spent battery energy. As the road grade becomes less and less negative, the motion of the vehicle is less assisted by gravity. Due to then increased dependence on motor power at this stage, the vehicle reuses its regenerated electrical energy momentarily to accelerate just enough to arrive at the destination timely. Finally, while decelerating in the end, the vehicle aims to maximise the energy it regenerates.

Mathematically, the evolution of co-states explains the cycle of increase in both the vehicle speed and the battery consumption followed by their decrease. Correlating the evolution of λ_{s} in Fig. 15 with the dynamics of λ_{k} described by (11), it is observed that first λ_{s} increases to limit the acceleration by decreasing λ_{k}, which in turn limits the propulsive power the motor provides as per (7), so that the vehicle begins to cruise quickly. When the vehicle must accelerate again after coasting, λ_{s} decreases significantly to momentarily increase the propulsive power P_{m} by increasing λ_{k}. This cycle is repeated for each set of crest followed by a trough on the road.

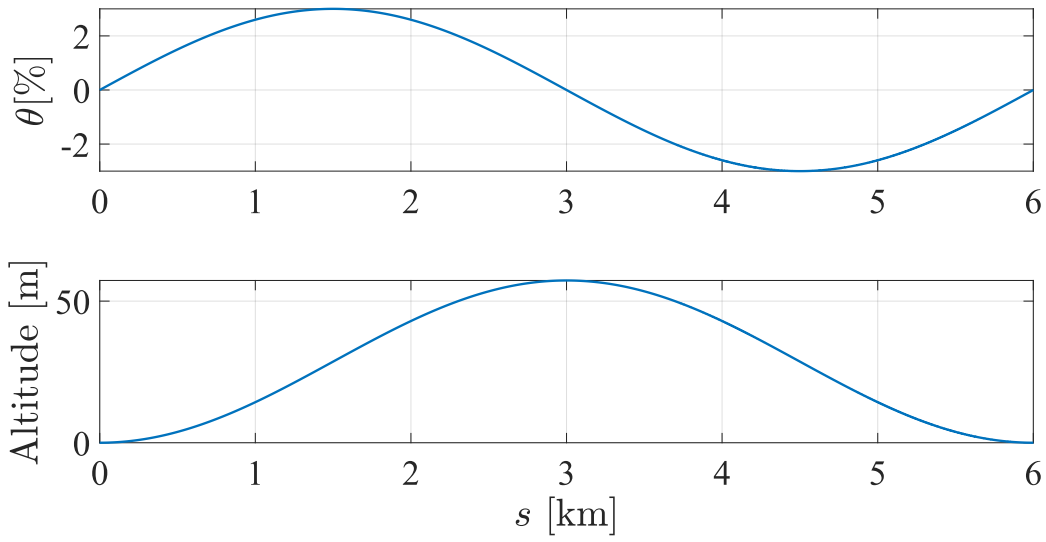

Fig. 13. Road profile used for the optimisation

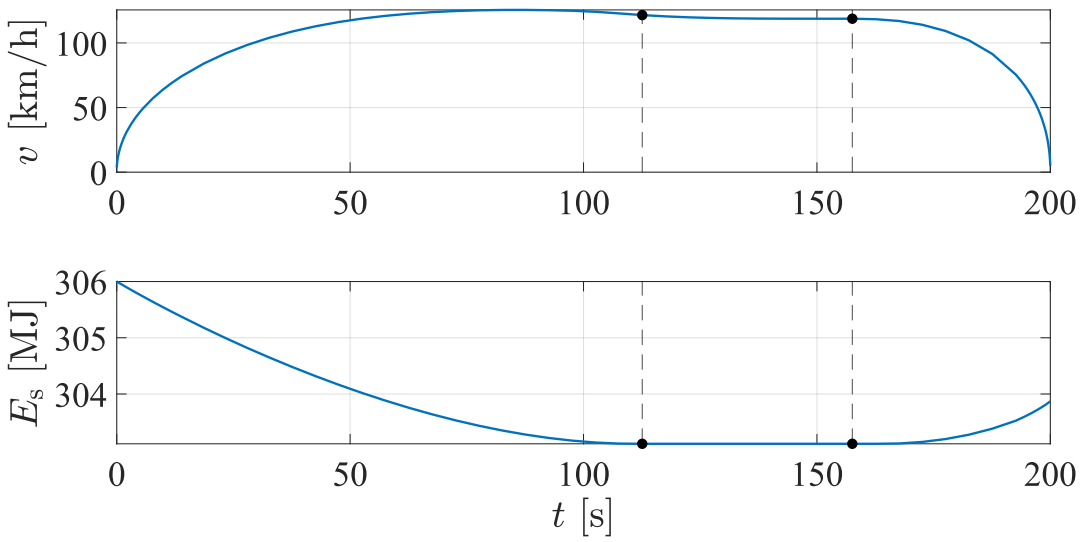

Fig. 14. Energy-optimal speed and battery state of energy trajectories for variable road grade

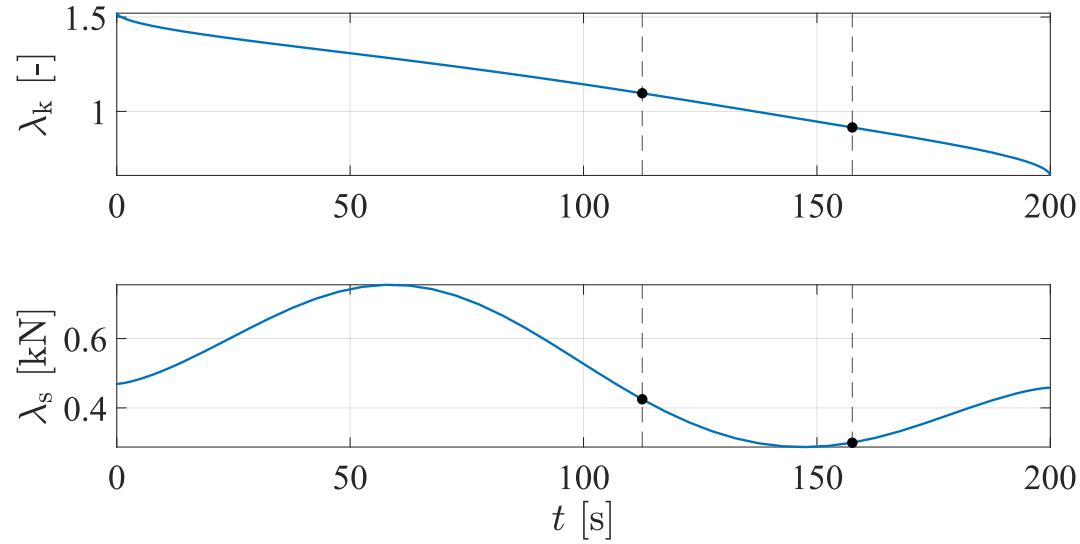

Fig. 15. Optimal co-state trajectories for variable road grade

Similarly, we analyse the case wherein the road goes first downhill and then uphill (refer Fig. 16). For such a road profile, the optimal speed trajectory and the corresponding consumption of stored battery energy is as in Fig. 17.

Here as well, the eco-driving system aims to maximise dependence on gravitationally assisted propulsion to minimise consumption of electrical energy stored in the battery. Interestingly, the vehicle passes two phases instead of one wherein the rate of change of battery state of energy stagnates. At $t = 0$ itself when the vehicle requires maximum propulsive power to accelerate, the acceleration due to gravity decreases the dependence of the vehicle on the motor to provide propulsive power. Consequently, the consumption of stored energy decreases sooner than for the road profile in Fig. 13. However, its regeneration towards the end is limited as the increasing road altitude offers greater resistance thereby increasing the dependence on the motors to provide power and hence consume energy.

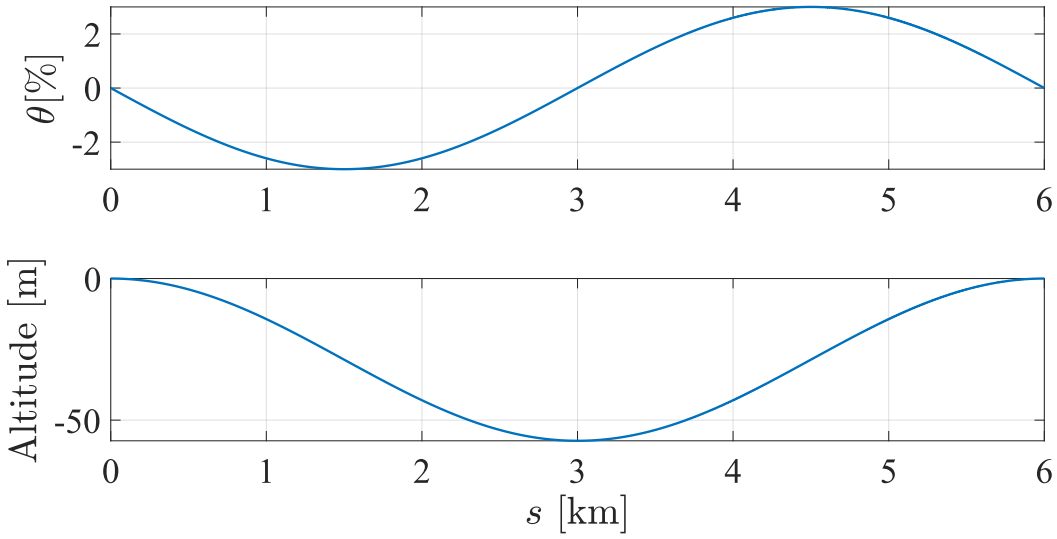

Fig. 16. Road profile used for simulation

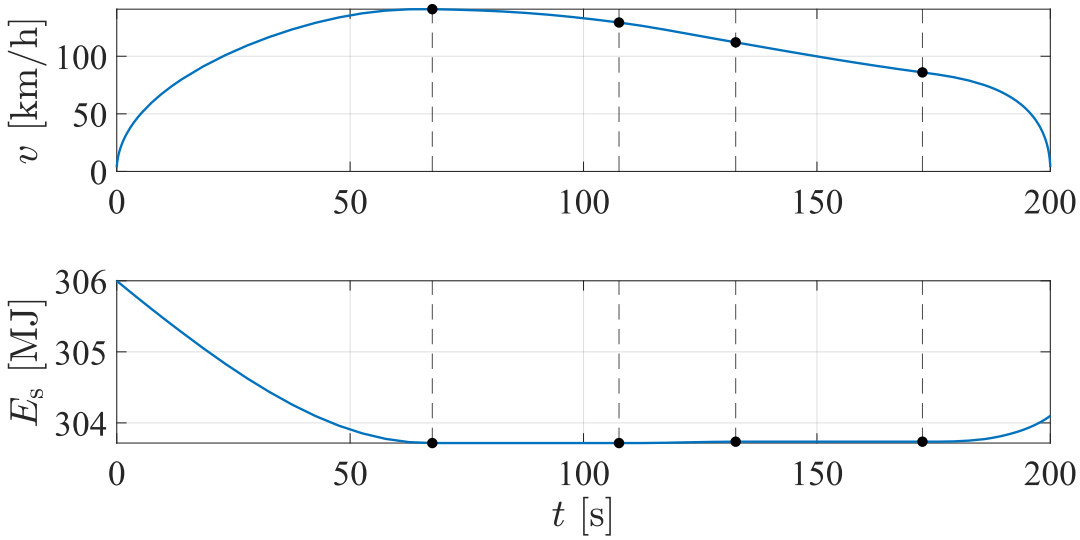

Fig. 17. Energy-optimal speed and battery state of energy trajectories for variable road grade

In conclusion from the driver's perspective, it is energy optimal to elongate the coasting phase whenever feasible to minimise the net consumption of battery energy by exploiting the added propulsive force by gravity when driving on roads with varying inclination.

The results obtained so far for different vehicle parameters and driving conditions are by application of PMP which is a locally optimal control method. Since the problem formulation is non-convex, it is essential to verify the global optimality of the results. To achieve this in the following chapter, the eco-driving problem in (4) subject to (7)–(11) is now recast in space domain and solved.

5

Convex Optimisation

In this chapter, we perform convexification of the original eco-driving problem (1) to compute globally optimal speed trajectories. Note that the two eco-driving problems we then have remain equivalent and can thus be used to optimise the speed trajectories for the same driving manoeuvre. The speed trajectories we obtain by solving the convex problem guarantee their global optimality and enable us to test the global optimality of the results generated by PMP following the solution method in Fig. 3.

The constraints and the state dynamics of the eco-driving problem we derive here are in terms of forces instead of powers, and formulated in space instead of time domain as in (1). The two modifications allow us to have only affine equality constraints and quadratic inequality constraints, making a second order conic programming problem solver applicable to solve the problem.

5.1 Problem Derivation and Constraints

The approach here is a simplification of that adopted by Borsboom et al. in [22] wherein the objective is to minimise the lap time of electric race cars subject to maximum available battery energy. Here, the objective is to minimise the expenditure of stored battery energy subject to maximum time. Mathematically, for a fixed increment of distance Δs and variable increment of time Δt, the eco-driving problem equivalent to that in (1) becomes:

$$
\begin{aligned}
\min_{F_{\mathrm{m},i},F_{\mathrm{d},i}} \quad & \sum_{i=1}^{s_\mathrm{f}/\Delta s} F_{\mathrm{s},i}\cdot\Delta s \\
\text{s.t.} \quad & E_\mathrm{k}(s+1) = E_\mathrm{k}(s) + \big(F_\mathrm{m}(s) - F_\mathrm{d}(s) - F_\mathrm{l}(s)\big)\cdot\Delta s \\
& E_\mathrm{s}(s+1) = E_\mathrm{s}(s) - F_\mathrm{s}(s)\cdot\Delta s \\
& t(s+1) = t(s) + \Delta t(s) \\
\text{and} \quad & E_\mathrm{k}(s=0) = E_\mathrm{k,o} \\
& E_\mathrm{k}(s=s_\mathrm{f}) = E_\mathrm{k,f} \\
& t(s=0) = 0 \\
& t\big(s=s_f\big) = T \\
& E_\mathrm{s}(s=0) = E_\mathrm{s,o}.
\end{aligned}
\tag{15}
$$

where F_l and F_s are force counterparts of P_l and P_s respectively. F_d and F_m are the two optimisation variables denoting the brake force and the propulsive force respectively.

To close the problem in (15), the variables E_k, E_s, F_s, t, Δt, F_m, F_d and F_l must be constrained. First, the constraints for the battery are derived. From the static circuit model [23], the powers before and after the internal losses of the battery are related as [22]

$$P_\mathrm{b} = P_\mathrm{s} - P_\mathrm{s}^2 \cdot \frac{R}{U_\mathrm{o}^2}. \tag{16}$$

Using the general relation $F = \frac{P}{v} = P \cdot \frac{\Delta t}{\Delta s}$, (16) in terms of forces is

$$F_\mathrm{b} \cdot \frac{1}{v} = F_\mathrm{s} \cdot \frac{1}{v} - F_\mathrm{s}^2 \cdot \frac{R}{U_\mathrm{o}^2}. \tag{17}$$

This equality constraint is, however, not affine and thus renders (15) non-convex. To maintain the convexity of the problem, (17) is relaxed as quadratic inequality as

$$\begin{aligned} F_\mathrm{b} \cdot \frac{1}{v} \leq F_\mathrm{s} \cdot \frac{1}{v} - F_\mathrm{s}^2 \cdot \frac{R}{U_\mathrm{o}^2} &\Leftrightarrow (F_\mathrm{s} - F_\mathrm{b}) \cdot \frac{1}{v} \geq F_\mathrm{s}^2 \cdot \frac{R}{U_\mathrm{o}^2} \\ &\Leftrightarrow (F_\mathrm{s} - F_\mathrm{b}) \cdot \frac{\Delta t}{\Delta s} \geq F_\mathrm{s}^2 \cdot \frac{R}{U_\mathrm{o}^2}. \end{aligned} \tag{18}$$

The inequality in (18) states that the internal losses of the battery are lesser than or equal to the absolute difference between the input and output battery (see Fig. 2). The optimisation algorithm maximises the power that the vehicle can withdraw from the battery to accelerate quickly to the cruising speed. This maximises the internal resistance loss of the battery and in turn holds (18) to an equality. Now, this is a constraint of the form $x_1 \cdot x_2 \geq x_3^2$ with x_1, x_2 and x_3 as constraint variables. Here, $x_1 = (F_\mathrm{s} - F_\mathrm{b})$, $x_2 = \frac{\Delta t}{\Delta s}$ and $x_3 = \frac{\sqrt{R}}{U_0} \cdot F_\mathrm{s}$. We formulate (18) as a second order conic constraint as in [24]

$$(F_\mathrm{s} - F_\mathrm{b}) \cdot \frac{1}{F_\mathrm{o}} + \frac{\Delta t}{\Delta s} \cdot v_\mathrm{o} \geq \left\| \begin{matrix} 2 \cdot \frac{\sqrt{R}}{U_0} \cdot F_\mathrm{s} \cdot \sqrt{\frac{v_\mathrm{o}}{F_\mathrm{o}}} \\ (F_\mathrm{s} - F_\mathrm{b}) \cdot \frac{1}{F_\mathrm{o}} - \frac{\Delta t}{\Delta s} \cdot v_\mathrm{o} \end{matrix} \right\|_2, \tag{19}$$

where $F_\mathrm{o} = 1\mathrm{N}$ and $v_o = 1\mathrm{m/s}$ are the normalisation coefficients. The battery power after the internal resistance losses is related to the power output of the motor as

$$P_{\mathrm{b}} = \frac{P_{\mathrm{m}}}{\eta_{\mathrm{m}}^{\mathrm{sgn}(P_{\mathrm{m}})}}. \tag{20}$$

Again, in terms of forces and splitting the constraint for the two cases related to $\mathrm{sgn}(P_{\mathrm{m}})$

$$F_{\mathrm{b}} = \begin{cases} \dfrac{F_{\mathrm{m}}}{\eta_{\mathrm{m}}} & F_{\mathrm{m}} \geq 0 \\ \eta_{\mathrm{m}} \cdot F_{\mathrm{m}} & F_{\mathrm{m}} < 0 \end{cases}. \tag{21}$$

To maintain convexity, this discontinuous constraint is relaxed as

$$\begin{aligned} F_{\mathrm{b}} &\geq \frac{F_{\mathrm{m}}}{\eta_{\mathrm{m}}}, \\ F_{\mathrm{b}} &\geq \eta_{\mathrm{m}} \cdot F_{\mathrm{m}}. \end{aligned} \tag{22}$$

Since increasing F_{b} arbitrarily violates the objective of minimising the net consumption of the battery power, F_{b} minimises to the ratio of F_{m} to η_{m} during acceleration and to their product during deceleration. Second, after the battery constraints, the input constraints are formulated for the motor power and the brake power. The instantaneous force counterpart of motor power F_{m} is bounded by maximum and minimum motor power as

$$\underline{P}_{\mathrm{m}} \cdot \Delta t(s) \leq F_{\mathrm{m}}(s) \cdot \Delta s \leq \bar{P}_{\mathrm{m}} \cdot \Delta t(s), \tag{23}$$

and the brake force is limited by maximum brake power as

$$0 \leq F_{\mathrm{d}}(s) \cdot \Delta s \leq \bar{P}_{\mathrm{d}} \cdot \Delta t(s). \tag{24}$$

The expression $\frac{\Delta s}{\Delta t(s)}$ is simply the discrete space approximation of instantaneous velocity $v(s)$. Thirdly, this expression is used to formulate the physical constraints. Each of the time increments Δt is related with the corresponding velocity as

$$v(s) \cdot \frac{\Delta t(s)}{\Delta s} = 1, \tag{25}$$

which is relaxed for convexity as $v(s) \cdot \frac{\Delta t(s)}{\Delta s} \geq 1$ and, similar to (19), represented as the second order conic constraint

$$\frac{\Delta t(s)}{\Delta s} \cdot v_{\mathrm{o}} + v(s) \cdot \frac{1}{v_{\mathrm{o}}} \geq \left\| \frac{\Delta t(s)}{\Delta s} \cdot v_{\mathrm{o}} - v(s) \cdot \frac{1}{v_{\mathrm{o}}} \right\|_2^2. \tag{26}$$

To minimise the quantisation error, the maximum time increment is bound. Moreover, increasing v arbitrarily consumes more stored electrical energy than optimal. Hence, the expression on the LHS of (26) is minimised such that the constraint will hold with an equality. The next physical constraint is for the persistent rolling resistance and aerodynamic drag the vehicle is subject to, and which is analogous to (9) and equals to

$$F_{\mathrm{l}} = \frac{\rho \cdot A \cdot c_d}{m} \cdot E_{\mathrm{k}} + m \cdot g \cdot (\sin\theta + c_{\mathrm{r}} \cdot \cos\theta). \tag{27}$$

Lastly, the state constraints are introduced to meet the time boundary condition and constrain kinetic energy. In order that the vehicle covers the distance s in time T,

$$\sum_{i=1}^{s_{\mathrm{f}}/\Delta s} (\Delta t)_i = T. \tag{28}$$

Finally, to bound the kinetic energy with instantaneous velocity,

$$E_{\mathrm{k}} = \frac{1}{2} \cdot m \cdot v^2. \tag{29}$$

with the convex relaxation

$$E_{\mathrm{k}} \geq \frac{1}{2} \cdot m \cdot v^2. \tag{30}$$

Similar to (26), maintaining a higher average kinetic energy of the vehicle over the whole trip duration consumes more stored electrical energy than optimal. Hence, with the objective to minimise its consumption, (30) will also hold with an equality.

5.2 Solution and Comparison with PMP Results

Here, we parse the optimisation problem (15) subject to the constraints (19), (22)–(24), (26)–(28) and (30) using YALMIP [25] for convenient expression of the problem into its standard

form. Gurobi is an appropriate second order conic programming solver freely available for academia [26] on which Yalmip can externally rely. Hence, we choose this solver.

Before solving, we take the following two steps to prevent numerical instabilities:

1. Scale the problem the ratio of the largest to the smallest numerical coefficient close to unity, and
2. Provide the variables without any direct physical bounds such as instantaneous velocity and resistive force with large bounds

Fig. 18 shows the energy-optimal speed trajectories we obtain on solving the equivalent problems (1) and (15) via PMP and convex optimisation respectively using the same numerical integration scheme of Euler forward method for both the optimal control methods for accurate comparison. To minimise the quantisation error in (15), we finely discretise the one-dimensional grid in 8001 points using $\Delta s = 0.75\text{m}$. The grid size required 1452.87s to solve. This time is 131.96 times larger than 11.01s which PMP required with a grid size of 113 points.

The resultant normalised root mean squared error (NRMSE) for the speed trajectory is 1.26%. And on comparing the battery state of energy at final time that we obtain from both PMP and convex optimisation, we calculated the percentage error of 0.06%. We explain these errors as follows: Solving (1) by PMP, the state, input and physical constraints hold with equalities, i.e. no constraint tolerances exist up to the default precision of Matlab. In convex optimisation of (15), we manually define the constraint tolerances up to which the linear and the quadratic constraints are allowed to violate. We observed reduced error on application of the variable precision toolbox to convex optimisation. However, we did not employ it to generate the final speed trajectory due to the requirement of higher computation power.

Hence, given the stated NRMSE and percentage errors for the speed trajectory that we obtained via application of PMP and convex optimisation, we conclude global optimality for the results generated by PMP. This makes PMP suitable for computing the globally optimal speed trajectories for near-straight line driving manoeuvres. For these manoeuvres, we expect these

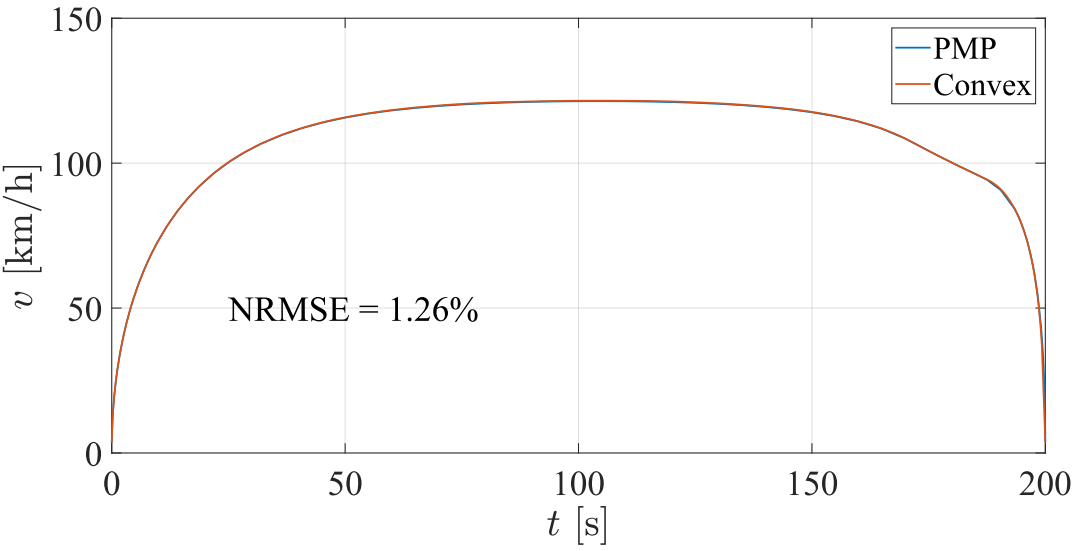

Fig. 18. Energy-optimal speed trajectories generated by PMP and convex optimisation for a regularly loaded vehicle driving on flat roads

speed trajectories, in theory, to consume the least amount of stored energy in the battery thereby achieving our goal of maximising the energy economy of EVs.

6

Conclusion and Future Work

To increase the energy savings in the transport sector via more frequent application of eco-driving system, we proposed a solution method to optimise speed trajectories for an originally non-convex eco-driving problem. The solution method is independent of the vehicle loading conditions, the distance to be travelled and the road grade. This generality allows for more frequent application of eco-driving system leading to greater energy savings.

We studied the energy-optimal state and co-state trajectories to generate energy-aware driving advice for the near-straight line driving manoeuvre. For increasing vehicle mass, smoother accelerations and decelerations leading to higher peak velocities was energy-optimal, for the increasing distances to be covered, it was optimal to maintain higher velocities throughout the trip duration, while for the increasing positive constant road grades, it was optimal to accelerate and decelerate faster to maintain lower cruising speeds. For all the cases, the cruising phase depleted the battery the most and it was beneficial to minimise the cruising velocities to minimise the total consumption of the stored electrical energy in the battery. This is in line with the conclusion of [10]. The strategy to minimise the expenditure of the battery energy in the case of variable road grades was to maximise the duration of the coasting phase in which the vehicle draws no power from the battery and regenerates while travelling downhill.

In the end, we tested the global optimality of the speed trajectories generated by PMP by convexification of the original eco-driving problem followed by convex optimisation. Within the calculated NRMSE for the speed trajectory and the percentage error for the final battery state of energy, the globally optimal results generated by convex optimisation matched with those generated by PMP proving its global optimality. Hence, for near-straight line driving manoeuvres, PMP is a computationally efficient control method to optimise speed trajectories for eco-driving. This is one of the ways to maximise the energy economy of on-road EVs through more a judicious utilisation of electrical energy generated by natural resources.

For future work: the optimisation of speed trajectory to implement eco-driving system in the vehicles here assumes it will yield energy savings by modifying the driver behaviour when implemented in the vehicles. However, the energy savings are rather limited due to the failure of the driver to exactly trace the energy-optimal speed trajectory. Hence, further robustification of the eco-driving problem to the real-time difference between the advised speed and the driver response by incorporating driver into the loop, i.e. generating real-time advice as a feedback to the driver's response, is a possible extension.

Appendix

Pontryagin's Minium Principle with Constraints

Consider the optimal control problem

$$\begin{aligned} \min_{u} \quad & \int_0^T g(x,u,t) + \Psi_{X(t)}(x) + \Psi_{U(t)}(u)\mathrm{d}t + h\big(x(T)\big) + \Psi_{X_f}\big(x(T)\big) \\ \text{s.t.} \quad & \dot{x}(t) = f(x,u,t)\ \forall t \in [0,T] \\ & x(0) = x_0 \\ \text{and} \quad & x(t) \in X(t) \\ & u(t) \in U(t) \\ & x(T) \in X_f, \end{aligned} \tag{31}$$

with state variables as x, and their initial values x_0 at time instant $t = 0$. The state dynamics, governed by f with respect to time, is a function of the state variables x, the control inputs u and the time t. X, U and X_f are the sets within which the states, the control inputs and the terminal states are contained respectively. The objective function consists of two parts: First, the integral of the algebraic sum of stage cost g and, the indicator functions defined for the state and the input constraints, i.e. $\Psi_{X(t)}$ and $\Psi_{U(t)}$ respectively. Two, the algebraic sum of end cost h and indicator function for terminal state. The indicator function is defined as

$$\Psi_Z(z) = \begin{cases} 0 & z \in Z \\ \infty & \text{else.} \end{cases} \tag{32}$$

To minimise the integral over a time horizon T, define the Hamiltonian

$$H(x,u,\lambda) = g(x,u,t) + \Psi_{X(t)}(x) + \Psi_{U(t)}(u) + \lambda^T \cdot f(x,u,t), \tag{33}$$

with the co-state variables λ and their dynamics as

$$\begin{aligned} & \dot{\lambda}(t) \in -\frac{\partial H}{\partial x}\Big|_* \text{ and} \\ & \lambda(T) \in -\frac{\partial h}{\partial x(T)}\Big|_* + N_{X_f}\big(x^*(T)\big), \end{aligned} \tag{34}$$

where $N_{X_f}\left(x^*(T)\right)$ is a normal cone, which, here, is the sub-differential of the indicator function $\Psi_{X_f}\left(x^*(T)\right)$. The asterisk denotes the optimal solution. Then the necessary conditions for optimality are given by

$$u^*(t) = \arg\min_u H\left(x^*(t), u, \lambda(t)\right), \tag{35}$$

Or

$$\left.\frac{\partial H}{\partial u}\right|_* = 0, \tag{36}$$

if H is convex [27].

Bibliography

[1] A. Sciarretta, G. De Nunzio, and L. L. Ojeda, “Optimal Ecodriving Control: Energy-Efficient Driving of Road Vehicles as an Optimal Control Problem,” *IEEE Control Systems*, vol. 35, no. 5, pp. 71–90, 2015, doi: 10.1109/MCS.2015.2449688.

[2] A. Cornet, R. Heuss, A. Tschiesner, R. Hensley, P. Hertzke, T. Möller, P. Schaufuss, J. Conzade, S. Schenk and K. von Laufenberg, “Why the automotive future is electric,” no. September, 2021, [Online]. Available: https://www.mckinsey.com/industries/automotive-and-assembly/our-insights/why-the-automotive-future-is-electric#.

[3] J. N. Barkenbus, “Eco-driving: An overlooked climate change initiative,” *Energy Policy*, vol. 38, no. 2, pp. 762–769, 2010, doi: https://doi.org/10.1016/j.enpol.2009.10.021.

[4] Y. Huang, E. C. Y. Ng, J. L. Zhou, N. C. Surawski, E. F. C. Chan, and G. Hong, “Eco-driving technology for sustainable road transport: A review,” *Renewable and Sustainable Energy Reviews*, vol. 93, pp. 596–609, 2018, doi: https://doi.org/10.1016/j.rser.2018.05.030.

[5] B. de Jager, T. A. C. van Keulen, and J. Kessels, *Optimal Control of Hybrid Vehicles*, 1st ed. Springer, London, 2013.

[6] R. Farrington and J. Rugh, “Impact of Vehicle Air-Conditioning on Fuel Economy, Tailpipe Emissions, and Electric Vehicle Range: Preprint,” [Online]. Available: https://www.osti.gov/biblio/764573.

[7] D. Pevec, J. Babic, A. Carvalho, Y. Ghiassi-Farrokhfal, W. Ketter, and V. Podobnik, “Electric Vehicle Range Anxiety: An Obstacle for the Personal Transportation (R)evolution?,” in *2019 4th International Conference on Smart and Sustainable Technologies (SpliTech)*, 2019, pp. 1–8, doi: 10.23919/SpliTech.2019.8783178.

[8] J. A. Sanguesa, V. Torres-Sanz, P. Garrido, F. J. Martinez, and J. M. Marquez-Barja, “A Review on Electric Vehicles: Technologies and Challenges,” *Smart Cities*, vol. 4, no. 1, pp. 372–404, 2021, doi: 10.3390/smartcities4010022.

[9] M. Salazar, P. Elbert, S. Ebbesen, C. Bussi, and C. H. Onder, “Time-optimal Control Policy for a Hybrid Electric Race Car,” *IEEE Transactions on Control Systems Technology*, vol. 25, no. 6, pp. 1921–1934, 2017, doi: 10.1109/TCST.2016.2642830.

[10] T. Van Keulen and M. Salazar, “Singular Fuel-optimal Control of the Velocity and Power-split of Hybrid Electric Vehicles via Pontryagin’s Minimum Principle,” *2021 IEEE Vehicle Power and Propulsion Conference, VPPC 2021 - ProceedingS*, Jul. 2021, doi: 10.1109/VPPC53923.2021.9699272.

[11] R. Bellman, “Dynamic Programming,” *Science*, vol. 153, no. 3731, pp. 34–37, 1966, doi: 10.1126/science.153.3731.34.

[12] E. Hellström, J. Åslund, and L. Nielsen, “Design of an efficient algorithm for fuel-optimal look-ahead control,” *Control Engineering Practice*, vol. 18, no. 11, pp. 1318–1327, 2010, doi: https://doi.org/10.1016/j.conengprac.2009.12.008.

[13] R. K. Kamalanathsharma and H. A. Rakha, “Multi-stage dynamic programming algorithm for eco-speed control at traffic signalized intersections,” in *16th International IEEE Conference on Intelligent Transportation Systems (ITSC 2013)*, 2013, pp. 2094–2099, doi: 10.1109/ITSC.2013.6728538.

[14] Z. Ye, K. Li, M. Stapelbroek, R. Savelsberg, M. Günther, and S. Pischinger, “Variable Step-Size Discrete Dynamic Programming for Vehicle Speed Trajectory Optimization,” *IEEE Transactions on Intelligent Transportation Systems*, vol. 20, no. 2, pp. 476–484, 2019, doi: 10.1109/TITS.2018.2812921.

[15] F. Zhang, L. Wang, S. Coskun, H. Pang, Y. Cui, and J. Xi, “Energy Management Strategies for Hybrid Electric Vehicles: Review, Classification, Comparison, and Outlook,” *Energies*, vol. 13, no. 13, 2020, doi: 10.3390/en13133352.

[16] W. Dib, A. Chasse, P. Moulin, A. Sciarretta, and G. Corde, “Optimal energy management for an electric vehicle in eco-driving applications,” *Control Engineering Practice*, vol. 29, pp. 299–307, 2014, doi: https://doi.org/10.1016/j.conengprac.2014.01.005.

[17] E. Ozatay, U. Ozguner, and D. Filev, “Velocity profile optimization of on road vehicles: Pontryagin’s Maximum Principle based approach,” *Control Engineering Practice*, vol. 61, pp. 244–254, 2017, doi: https://doi.org/10.1016/j.conengprac.2016.09.006.

[18] “Bellman’s Principle of Optimality and its Generalizations,” in *General Systems Theory: A Mathematical Approach*, Boston, MA: Springer US, 2002, pp. 135–161.

[19] B. Du, L. Zhang, J. Zou, J. Han, Y. Zhang, and H. Xu, “Investigating the impact of route topography on real driving emission tests based on large data sample at data window level,” *Science of The Total Environment*, vol. 809, p. 151133, 2022, doi: https://doi.org/10.1016/j.scitotenv.2021.151133.

[20] M. V Faria, G. O. Duarte, R. A. Varella, T. L. Farias, and P. C. Baptista, “How do road grade, road type and driving aggressiveness impact vehicle fuel consumption? Assessing potential fuel savings in Lisbon, Portugal,” *Transportation Research Part D: Transport and Environment*, vol. 72, pp. 148–161, 2019, doi: https://doi.org/10.1016/j.trd.2019.04.016.

[21] F. Kutzner, C. Kacperski, D. Schramm, and M. Waenke, “How far can we get with eco driving tech?,” *Journal of Environmental Psychology*, vol. 76, p. 101626, 2021, doi: https://doi.org/10.1016/j.jenvp.2021.101626.

[22] O. Borsboom, C. A. Fahdzyana, T. Hofman, and M. Salazar, “A Convex Optimization Framework for Minimum Lap Time Design and Control of Electric Race Cars,” *IEEE Transactions on Vehicular Technology*, vol. 70, no. 9, pp. 8478–8489, 2021, doi: 10.1109/TVT.2021.3093164.

[23] L. Guzzella and A. Sciarretta, *Vehicle Propulsion Systems*, 3rd ed. Springer Berlin, Heidelberg, 2013.

[24] M. Salazar, “Time-Optimal Control of the Formula 1 Hybrid Electric Power Unit,” ETH Zurich, Zurich.

[25] J. Lofberg, “YALMIP : a toolbox for modeling and optimization in MATLAB,” in *2004 IEEE International Conference on Robotics and Automation (IEEE Cat.*

No.04CH37508), 2004, pp. 284–289, doi: 10.1109/CACSD.2004.1393890.

[26] Gurobi Optimization, LLC, "Gurobi Optimizer Reference Manual." 2022, [Online]. Available: https://www.gurobi.com.

[27] S. Onori, L. Serrao, and G. Rizzoni, "Pontryagin's Minimum Principle," in *Hybrid Electric Vehicles: Energy Management Strategies*, London: Springer London, 2016, pp. 51–63.